Regular Article

ANALYTICAL AND BIOANALYTICAL CHEMISTRY RESEARCH

Published by the Iranian Chemical Society

Anal. Bioanal. Chem. Res., Vol. 9, No. 3, 281-291, July 2022.

Metoprolol Removal from Water Using Fe_3O_4/TiO_2/Activated Carbon Nanocomposite: Adsorption Isotherm, Kinetics and Thermodynamics

Amrollah Parsaie[a], Mohammad Reza Baezat[a,*] and Nadereh Rahbar[b]

[a]*Department of Chemistry, Payame Noor University, Tehran, Iran*

[b]*Nanotechnology Research Center, School of Pharmacy, Ahvaz Jundishapur University of Medical Sciences, Ahvaz, Iran*

(Received 27 August 2021 Accepted 16 January 2022)

Metoprolol (MTP), a selective beta-blocker with low biodegradability, is an important micro-pollutant that has been widely identified in surface waters and wastewaters. In this work, the removal of MTP from aqueous solutions was performed using Iron oxide/Titanium oxide/activated carbon (Fe_3O_4/TiO_2/AC) nanocomposite as a new adsorbent. The nanocomposite was characterized by Fourier Transform Infrared (FT-IR), Energy Dispersive X-ray Spectroscopy (EDX), Field Emission Scanning Electron Microscopy (FESEM) and X-Ray Diffraction (XRD) techniques. The maximum efficiency of MTP removal was 96.2% at a dosage of 1.5 g l^{-1} of adsorbent, an initial concentration of 10 mg l^{-1} of the drug, a contact time of 60 min at 25 °C, and pH 8.0. Freundlich and Pseudo-second-order models were found to be the best fitting isotherm and kinetic models, respectively. In addition, the values of thermodynamic parameters including ΔH, ΔS, and ΔG were found to be -75.20, -0.23, and -7.55 kJ mol^{-1}, respectively. These results confirmed that the adsorption process of MTP on Fe_3O_4/TiO_2/AC is exothermic and spontaneous. Fe_3O_4/TiO_2/AC nanocomposite was successfully used for the removal of MTP from real water solutions.

Keywords: Metoprolol, Iron oxide nanoparticles, Titanium oxide nanoparticles, Activated carbon, Adsorption

INTRODUCTION

Metoprolol (MTP), a common sympathetic blocker (Fig. 1), is used to treat cardiovascular diseases such as myocardial infarction, arrhythmia, and hypertension [1,2]. MTP has been frequently detected as a contaminant in surface waters and wastewaters due to its resistance to hydrolysis and widespread use [3-5]. This pollutant needs to be removed from wastewater before discharging it to ecosystem or water bodies due to its harmful impacts on the environment and human health [6-8].

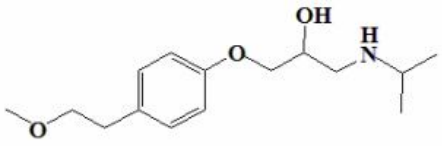

Fig. 1. Chemical structure of MTP.

Various strategies such as oxidation [9], photocatalytic [10-12], adsorption [13,14], filtration [15], and electrochemical [16] methods have been used for the elimination and the degradation of MTP from polluted water bodies. Adsorption is an attractive technique compared to other methods due to its cost-effectiveness, simple design, and straightforward approach [17,6]. This strategy has been extensively applied to remove organic materials from wastewater using different types of adsorbents such as natural materials, magnetic composites, activated carbon (AC), silica, and polymers [18-23]. However, the performance of the adsorption process strongly depends on the affinity between the surface of the adsorbent and the

*Corresponding author. E-mail: Mrbaezzat@pnu.ac.ir

contaminant, as well as the ease of separation of the adsorbent from the sample solution. Therefore, the development of adsorbents that can be easily separated from the aqueous solution and have a high affinity for MTP is highly desirable.

AC alone or in combination with other materials is widely used to eliminate various contaminants from polluted aqueous media due to its large surface area, microporous structure with high porosity, and suitable adsorption capacity [24-26]. In addition, magnetic nanoparticles have been used to absorb pollutants due to their large surface area, adsorption capacity, and easy separation from aqueous solutions by an external magnetic field [27-29]. In addition, TiO_2 is widely used as a catalyst in photocatalytic degradation processes to remove contaminants [9,10,30,31]. Although TiO_2 is commonly used alone in photocatalytic reactions, it is usually conjugated with other compounds for use in adsorption processes [32-35].

Due to the harmfulness of MTP to human health and the environment, further research is needed for the simple, rapid, and effective removal of this drug from aqueous solutions. Therefore, a nanocomposite with a combination of Fe_3O_4 nanoparticles, TiO_2 nanoparticles, and AC was introduced for the first time to increase the efficiency of the adsorption method in removing MTP by utilizing the special abilities of each adsorbent, such as easy adsorbent separation and high affinity for the drug. In order to achieve the optimal conditions for the adsorption process, the parameters influencing this process were investigated. Moreover, the behavior of the nanocomposite in the adsorption of MTP was evaluated by the isotherm, kinetic, and thermodynamic studies.

MATERIALS AND METHOD

Chemicals and Standards

Hydrochloric acid (HCl), Sodium hydroxide (NaOH), Iron(II) Chloride.$4H_2O$, Iron(III) Chloride.$6H_2O$, TiO_2 nanoparticles, and activated graphite powder were purchased from Merck (Darmstadt, Hesse, Germany). MTP standard was obtained from Sigma-Aldrich (St. Louis, Missouri, USA). A 200 mg l^{-1} solution stock of MTP was prepared by dissolving an equivalent amount of the standard drug in double-distilled water. NaOH and HCl solutions were used to adjust the pH of the MTP solutions.

Apparatus

The morphology of the studied nanocomposite was characterized by a Field Emission Scanning Electron Microscope (FESEM) and Energy Dispersive X-ray Diffraction (EDX) using a Tescan model Mira3-XMU instrument (Czech Republic). The Fourier transform infrared (FT-IR) spectra were recorded using a Bruker spectrometer (model Tensor 27, Germany). The pattern of the nanocomposite X-ray diffraction (XRD) was recorded using an X'Pert Pro MPD instrument (PANalytical, Netherlands). The magnetic properties of the synthesized Fe_3O_4 nanoparticles and Fe_3O_4/TiO_2/AC nanocomposite were investigated using a vibrating sample magnetometer (VSM) instrument (MDK-VSM, Meghnatis Daghigh Daneshpajouh Co., Iran). The UV-Vis spectrophotometer (PerkinElmer) was used to measure the residual concentration of MTP.

The Synthesis of Fe_3O_4/TiO_2/AC Nanocomposite

In the first step, 2 g $FeCl_2.4H_2O$ and 5.2 g $FeCl_3.6H_2O$ salts were dissolved in100 ml of deionized water and then, stirred at 80 °C for 10 min. Then, the pH of the solution was adjusted to 8.0 with a few drops of NaOH and HCl solutions, resulting in the formation of a thick black precipitate. The whole process was carried out under a nitrogen atmosphere [34]. A suitable magnet was used to separate the precipitate from the reaction medium. Fe_3O_4 precipitate was washed three times with distilled water and finally dried at ambient temperature. In the second step, 0.1 g of TiO_2 nanoparticles, 0.3 g of AC powder, and 0.4 g of Fe_3O_4 nanoparticles were mixed with 50 ml of distilled water under the vigorous stirring conditions at room temperature for 10 min. Then, a few drops of HCl solution (1 M) were added to the solution and the pH of the solution was adjusted to 8 using NaOH solution (0.5 M). The prepared adsorbent was heated at 80 °C for another 10 min. The resulting precipitate was separated from the suspension by a magnetic field, rinsed several times with distilled water, and finally dried in an oven at 120 °C for 24 h in the oven. This nanocomposite was used as an adsorbent for the removal of MTP from the aqueous solutions.

Adsorption Procedure

A known amount of Fe_3O_4/TiO_2/AC was added to 10 ml of MTP solution at the specified concentration and contact time, at 25 °C and stirring speed of 1000 rpm. After the separation of the adsorbent by a magnet, the concentration of the remaining MTP in solution was measured spectrophotometrically at 227 nm. The spectra for the MTP solution before and after adsorption with Fe_3O_4/TiO_2/AC are presented in Fig. 2. To ensure that the results are reliable, all experiments were performed twice and repeated a third time in case of uncertainties. The removal efficiency for MTP (%R) was calculated using Eq. (1):

$$R\% = \frac{(C_0 - C_e)}{C_0} \times 100 \quad (1)$$

In this equation, C_0 and C_e (mg l^{-1}) are the initial and equilibrium concentrations of MTP, respectively.

The amount of MTP adsorbed per unit mass of Fe_3O_4/TiO_2/AC nanocomposite (q_e, mg g^{-1}) at equilibrium condition can be calculated by Eq. (2):

$$q_e = \frac{(C_0 - C_t)}{M} \times V \quad (2)$$

where C_0 and C_t (mg l^{-1}) are the MTP concentrations are at zero and t times, respectively. V is the volume of the solution (l) and M is the weight of the adsorbent (g).

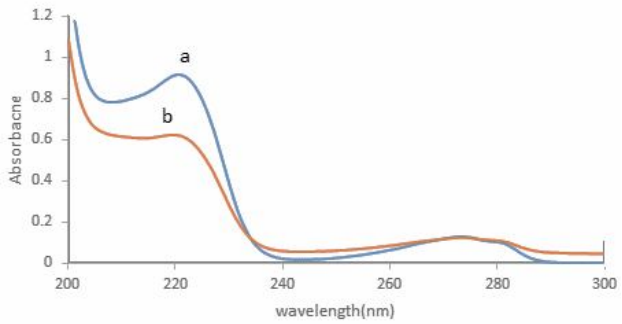

Fig. 2. UV-Vis spectra of MTP solution before (a) and after (b) exposure to the adsorbent (condition: MTP concentration, 10 mg l^{-1}; pH 8; the adsorbent amount, 0.5 g l^{-1}; contact time, 15 min), at λ_{max} = 227 nm).

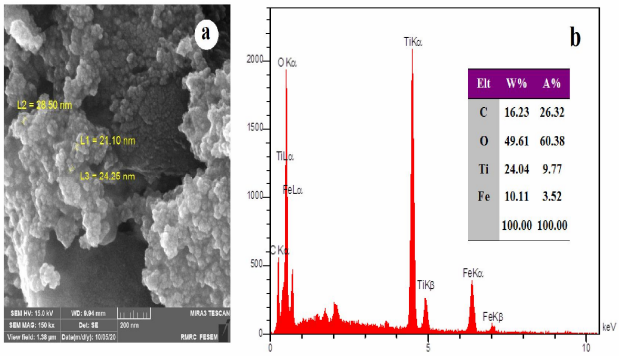

Fig. 3. EDX spectra (a) and FESEM images (b) of Fe_3O_4/TiO_2/AC nanocomposite.

RESULTS AND DISCUSSION

Characterization of Fe_3O_4/TiO_2/AC Nnanocomposite

The FESEM image of Fe_3O_4/TiO_2/AC nanocomposite confirmed the nearly spherical shape of the nanocomposite with diameters less than 50 nm (Fig. 3a). Moreover, the EDX spectrum confirmed the presence of oxygen, carbon, iron, and titanium elements as the constituents of the nanocomposite (Fig. 3b). As shown in Fig. 4, the detectable and sharp peaks of TiO_2, C and Fe_3O_4 are observed at 2θ values of about 25.5° (101 plane), 26.5° (002 plane) and 35.5° (311 plane), respectively, indicating their crystalline structure [36-38]. FTIR spectra of the nanocomposites are also shown in Fig. 5a. The strong bands at 620 and 579 cm^{-1} were assigned to the Ti–O and Fe–O bonds, respectively.

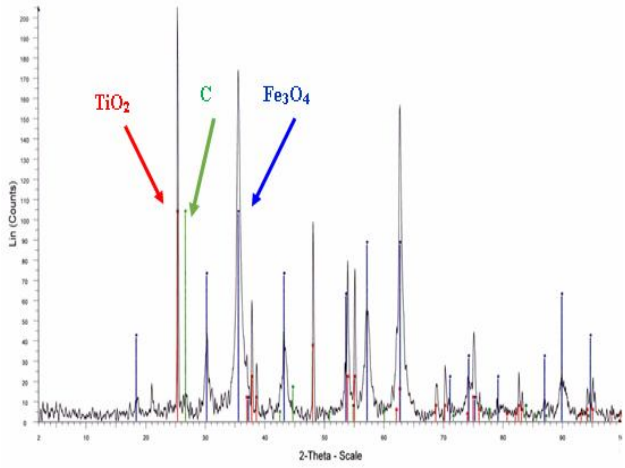

Fig. 4. XRD pattern of the Fe_3O_4/TiO_2/AC nanocomposite.

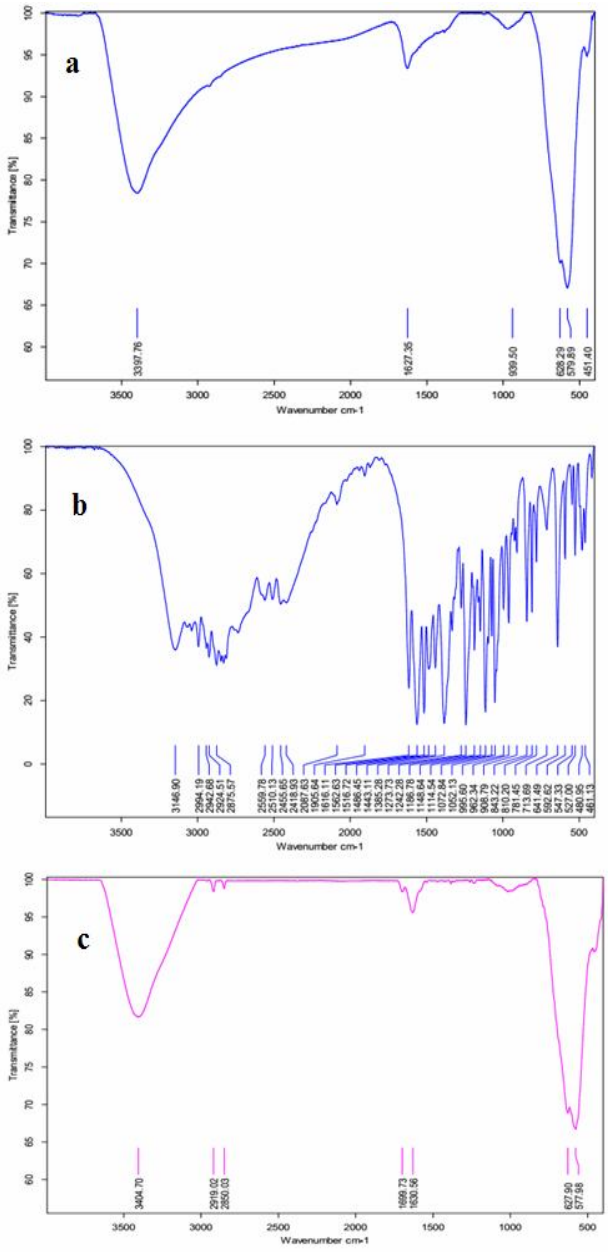

Fig. 5. FTIR spectra of (a) Fe_3O_4/TiO_2/AC nanocomposite (b) MTP, (c) MTP adsorbed on Fe_3O_4/TiO_2/AC nanocomposite.

The broad band around 3397 cm^{-1} can be related to the O–H group (symmetric and asymmetric stretching vibrations) while the band at about 1630 cm^{-1} is attributed to the bending vibrations of H–O–H on the incorporated activated carbon. The presence of the peaks at ~1562.63 and ~1114 cm^{-1} in FTIR spectrum of MTP (Fig. 5b) can be associated with the vibrations of the H-N bond and the bond O–C (in C–O–C functional group). In the area of 1443 cm^{-1} and 1385 cm^{-1}, there are some peaks related to C=C and C–H aromatic bonds, respectively. The peak in the area of 1062 cm^{-1} indicates the C–O bond of the first alcohol type while at 1516 cm^{-1} shows the aromatic ring. FTIR spectrum of MTP bound to the surface of Fe_3O_4/TiO_2/AC nanocomposite is shown in Fig. 5c. In this spectrum, there are two peaks in the region of 2580 cm^{-1} and 2919 cm^{-1} which are related to the aliphatic C-H bonds. The peak in the region of 1699 cm^{-1} indicates the aromatic C=C bond. The strong peak in the region of 3404 cm^{-1} is related to the N-H bond of the amine group. These results indicate that MTP was adsorbed on the surface of the new composite. The magnetic properties of Fe_3O_4 nanoparticles and Fe_3O_4/TiO_2/AC nanocomposite were investigated by VSM. As seen in Fig. 6, the absence of magnetic hysteresis loops in both curves indicates the superparamagnetic property of the magnetic nanocomposite (39]. Furthermore, the saturation magnetization of Fe_3O_4/TiO_2/AC (38.9 emu g^{-1}) is significantly lower than that of Fe_3O_4 nanoparticles (69.4 emu g^{-1}), indicating the existence of TiO_2 nanoparticles and AC as magnetic property reducing compounds. However, Fe_3O_4/TiO_2/AC nanocomposite was

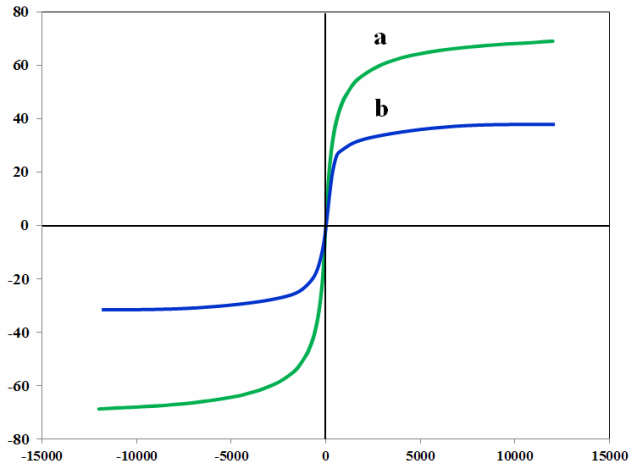

Fig. 6. VSM magnetization curves of (a) Fe_3O_4 nanoparticles and (b) Fe_3O_4/TiO_2/AC nanocomposite.

quickly separated from the sample solution by a magnet due to its relatively high saturation magnetization values.

Adsorption Experimental Conditions

Preliminary drug removal experiments were performed separately with each of the adsorbent components with 10 mg l^{-1} MTP solution and the adsorbent amount of 0.5 g l^{-1}, and the contact time of 15 min at pH of distilled water. The ability of Fe_3O_4 nanoparticles to adsorb MTP under the above conditions was investigated and it was found that the removal efficiency was negligible. Removal efficiency of about 56% was achieved by the addition of TiO_2. MTP was removed about 80% from the solution by the addition of AC. Therefore, it was concluded that the combination of TiO_2 and AC nanoparticles can improve the removal efficiency, indicating the synergistic effect of this composition. According to these results, the role of Fe_3O_4 nanoparticles in the composite might be mainly related to their ability to separate the composite from the sample solution after removal experiments in the presence of an external magnetic field. This is an excellent property of Fe_3O_4/TiO_2/AC nanocomposite. Suspended and non-magnetic titanium oxide nanoparticles, as well as graphite powder, can be separated with magnetite nanoparticles, indicating possible electrostatic or hydrogen bonding forces between the nanocomposite constituents. This phenomenon was not observed, for example, with a mixture of zirconia (ZrO_2) and Fe_3O_4 nanoparticles. ZrO_2 nanoparticles cannot be separated from the aqueous phase containing magnetite nanoparticles [39]. In addition, a dark removal experiment (MTP concentration of 10 mg l^{-1}, the adsorbent dosage of 0.5 g l^{-1}, and the contact time of 15 min at pH of distilled water) was performed to prove that photo-degradation of MTP with TiO_2 in daylight does not participate in the removal process. The results of this experiment showed that the difference between MTP removal efficiencies in dark and ambient light experiments was negligible.

Effect of pH. In the adsorption process, pH of the solution affects the degree of ionization of the surface charge of the adsorbent, and the removal efficiency [13-17]. Therefore, the effect of pH on the removal process was investigated in the range of 4-9 under the following condition: adsorbent amount, 0.5 g l^{-1}; MTP concentration, 10 mg l^{-1}; contact time, 15 min at 25 ºC. As shown in

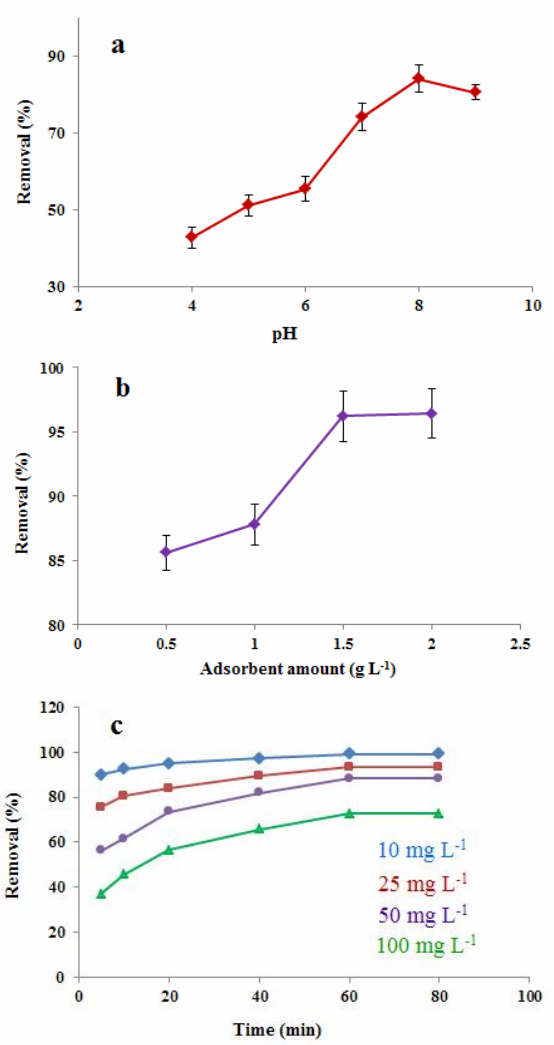

Fig. 7. The influence of (a) pH (condition: the adsorbent amount, 0.5 g l^{-1}; MTP concentration, 10 mg l^{-1}; contact time, 15 min at 25 ºC), (b) the adsorbent amount (condition: MTP concentration, 10 mg l^{-1}; pH 8.0; contact time, 15 min at 25 ºC), and (c) contact time (condition: the adsorbent amount, 1.5 g l^{-1}; pH 8.0 at 25 ºC) on the removal efficiency of MTP.

Fig. 7a, the removal efficiency of MTP gradually increases up to a pH of 8.0. Based on these results, the highest MTP removal efficiency (84.2%) was obtained at pH 8.0. It can be assumed that at high concentrations of H^+ (at acidic pH), the surface of the adsorbent has a positive

charge, which is probably due to the interaction between the hydrogen ions and the oxygen atoms of Fe_3O_4/TiO_2/AC nanocomposite. However, in highly acidic environments, most of the amine groups of MTP molecules are in the protonated form of $-NH_3^+$, and therefore the repulsive forces between these ammonium groups and the positively charged adsorbent surface reduce the removal percentage. As the pH increases, the number of amine groups increases and the positive charge of the surface of the adsorbent decreases. Under this condition, the removal efficiency improves in the presence of hydrogen bonding and electrostatic attraction between the MTP amine groups and the adsorbent surface containing oxygen atoms and metal cations. In other words, in addition to the penetration of MTP molecules into carbon cavities by physical adsorption, the formation of a complex between the titanium and amine groups of MTP can be assumed. However, at pH values above 8, the removal efficiency decreases due to the repulsive forces between the basic amine groups of MPT and the –OH groups covering the adsorbent.

Effect of the adsorbent amount. The effect of adsorbent dose (0.5-2.0 g l^{-1}) was studied to determine the optimum amount of the nanocomposite in order to achieve the best removal efficiency. These experiments were conducted under the following conditions: 10 ml of MTP solution (10 mg l^{-1}), solution pH = 8.0, stirring time of 15 min at 25 ºC. The results are shown in Fig. 7b. It is clear that the removal efficiency of the drug increases with increasing the adsorbent amount from 0.5 to 1.5 g l^{-1}, due to the availability of larger absorbable surfaces for MTP molecules [40]. However, an increase in adsorbent dose and hence, increasing removal efficiency leads to a decrease in adsorption capacity [14]. The removal percentage of MTP was increased up to an adsorbent dosage of 1.5 g l^{-1}, and then the equilibrium condition was reached with a maximum removal percent of 92.6%. Therefore, the adsorbent dosage of 1.5 g l^{-1} was selected as the optimum value.

Effects of contact time and initial concentration of MTP. The effect of contact time in the range of 5-80 min for different concentrations of MTP in the range of 10 to 100 mg l^{-1} was investigated under the following condition: solution pH of 8.0, adsorbent amount of 1.5 g l^{-1}, and ambient temperature of 25 °C. The results (Fig. 7c) showed that as the initial concentration of MTP increased, the removal efficiency of the drug decreased and the adsorption of MTP on the nanocomposite reached the equilibrium condition after 60 min at all concentrations. On the other hand, the highest removal efficiency was obtained at MTP concentration of 10 mg l^{-1} (96.2%).

Sorption Isotherms

The sorption isotherms of MTP on Fe_3O_4/TiO_2/AC were studied using four isotherm models, namely Langmuir, Freundlich, Temkin, and Dubinin-Radushkevich (D-R) and their linear equations are defined in Eqs. ((3)-(6)), respectively:

$$C_e/q_e = 1/(q_m K_L) + C_e/q_m \quad (3)$$

$$\log q_e = \log K_F + 1/n \log C_e \quad (4)$$

$$q_e = B \ln K_T + B \ln C_e \quad (5)$$

$$\ln q_e = \ln q_m - D\varepsilon^2 \quad (6)$$

where C_e (mg l^{-1}), q_e (mg g^{-1}) and q_m (mg g^{-1}) are the equilibrium concentration of the adsorbate, the amount of equilibrium adsorption, and the maximum value of adsorption capacity, respectively. K_L (l mg^{-1}), K_F (mg g^{-1}), n (mg l^{-1}) and, R_L ($1/(1 + C_0 K_L)$) are the Langmuir constant, Freundlich equilibrium constant, the desirability extent of adsorption procedure, and the separation parameter, respectively. In general, the desirability of the adsorption process can be indicated R_L ($0 < R_L < 1$). Moreover, in D-R model, ε (kJ mol^{-1}) is the Polanyi potential and can be determined *via* $\varepsilon = RT \ln(1 + (1/Ce))$ equation. The value of E (kJ mol^{-1}) called the mean free energy of adsorption in D-R model can be calculated with the equation $E = 1/(-2D)^{-0.5}$.

The monolayer adsorption of adsorbate on a surface of homogeneous adsorbent can be described in the context of Langmuir isotherm. Freundlich isotherm model is defined on the basis of multilayer adsorption on a heterogeneous surface of the adsorbent with unequal energies. Moreover, the D-R isotherm model shows a surface with homogeneous adsorption energy and the indirect interactions between the adsorbent and the adsorbent are investigated in the Temkin model. The parameters of the isotherm for all models and

Table 1. The Obtained Parameters Related to the Various Isotherm Models for MTP Adsorption

Models	Parameters	Values
Isotherm		
Langmuir	q_m (mg g^{-1})	25.316
	K_L (l mg^{-1})	0.239
	R_L	0.077
	R^2	0.968
Freundlich	K_F (l mg^{-1})	6.426
	1/n	0.416
	R^2	0.999
Dubinin-Radushkevich (D-R)	q_m (mg g^{-1})	16.615
	D (mol^2 $(kJ^2)^{-1}$)	-0.2868
	E (kJ mol^{-1})	1.321
	R^2	0.8109
Temkin	B	4.956
	K_T	3.246
	R^2	0.958

Table 2. The Obtained Parameters Related to the Various Kinetic Models for MTP Adsorption

Models	Parameters	Values
Kinetic		
Pseudo-first order	$q_{1,cal.}$ (mg g^{-1})	5.851
	K_1 (min^{-1})	4.803
	R^2	0.964
Pseudo-second order	$q_{2,cal.}$ (mg g^{-1})	6.618
	K_2 (g mg^{-1} min^{-1})	0.0193
	R^2	0.993
Elovich	α (mg g^{-1} min^{-1})	2.296
	β (g mg^{-1})	1.156
	R^2	0.993
Intra-particle diffusion	K_{ip} (mg g^{-1} $min^{0.5}$)	0.518
	C_i (mg g^{-1})	2.0656
	R^2	0.9858
Experimental	$q_{e, Exp.}$	

their linear plots are given in Table 1 and Figs. S1-S4 (in the supplementary information) by fitting the experimental data. According to the obtained data, the sorption of MTP on the Fe_3O_4/TiO_2/AC nanocomposite is better fitted to the Freundlich model (R^2 = 0.999). These results show that the surface of the adsorbent is heterogeneous, and also has different and non-uniform energy values. In the Freundlich equation, 1/n can describe the favorability of the adsorption process. Values of n in the range of 1-10 as well as 1/n less than 1 confirm the suitability of the adsorption process. As can be seen from Table 1, the small value of 1/n (0.416), which ranges from 0 to 1, and the large value of K_F (6.426) indicate that MTP is effectively adsorbed by Fe_3O_4/TiO_2/AC nanocomposite. Therefore, it can be concluded that the adsorption process could be carried out *via* chemical sorption as a process-limiting step [35,41].

Kinetic Modeling

Sorption kinetics was also investigated to identify the mechanism of MTP adsorption on the prepared nanocomposite. For this purpose, four kinetic models including pseudo-first-order (Eq. (7)), pseudo-second-order (Eq. (8)), intra-particle diffusion (Eq. (9)), and Elovich (Eq. (10)), were used to investigate the mechanism of the adsorption process, whose equations are as follows:

$$1/q_t = k_1/q_1 t + 1/q_1 \quad (7)$$

$$t/q_t = t/q_2 + 1/k_2 q_2^2 \quad (8)$$

$$q_t = k_{ip}\, t^{0.5} + C_{ip} \quad (9)$$

$$q_t = \beta \ln(\alpha\beta) + \beta \ln t \quad (10)$$

where q_t, is the adsorption capacity at a given time t, and q_1, and q_2 are the adsorption capacity at equilibrium state for pseudo-first-order and pseudo-second-order kinetic models, respectively. The rate constants of pseudo-first-order, pseudo-second-order, and intra-particle diffusion kinetic models are k_1, k_2, and k_{ip} are, respectively. The obtained kinetic parameters for all models and their linear graphs are presented in Table 2 and Figs. S5-S8 (in supplementary information) by fitting the experimental data. As can be seen, the pseudo-second-order model was found to be the

best model for fitting the experimental data. Therefore, it can be concluded that the adsorption process may be performed via chemical adsorption as a limiting step [42].

Effect of Temperature: Determination of Thermodynamics Parameters

The effect of solution temperature on the adsorption efficiency in the range of 25-60 ºC under the optimum conditions, including solution pH of 8, MTP concentration of 10 mg l^{-1}, the adsorbent dose of 1.5 mg l^{-1}, and the contact time of 60 min, was investigated. Based on the obtained results, the optimum temperature for MTP adsorption and also the corresponding thermodynamic parameters were determined. The results clearly showed that at temperatures above 25 °C, the removal efficiency of MTP gradually decreased, indicating that lower temperatures are suitable for the adsorption process (Fig. S9). The thermodynamic parameters such as standard entropy change standard enthalpy change (ΔH°, kJ mol^{-1}), (ΔS°, kJ mol^{-1} K^{-1}), and Gibbs energy (ΔG°, $kJmol^{-1}$) were determined using the following equations [42]:

$$\Delta G° = -RTLnK_d \quad (11)$$

$$\Delta G° = \Delta H° - T\Delta S° \quad (12)$$

In Eq. (11) (Van't Hoff equation) K_d and T are distribution coefficient of the sorption process (which can be calculated by the ratio of the adsorbed MTP concentration to the aqueous phase MTP concentration) and the absolute temperature (K), respectively. The linear plot of Van't Hoff equation is presented in Fig. S10. As shown in Table 3, the negative value for ΔG° at all temperatures demonstrates the sorption process spontaneity. In addition, a negative value of ΔH° indicates the exothermic nature of the adsorption process. Negative values of ΔG° and ΔH° together with increasing value of ΔG° with increasing temperature indicate that the reaction at low temperature is more favorable [43,44].

Comparison with other Sorbents

Some characteristics of the adsorption process in the removal of MTP by Fe_3O_4/TiO_2/AC nanocomposites including q_m, pH, temperature and R% were compared with the results reported in the literature using other adsorbents, as presented in Table 4. The features of the proposed method are in some cases better or comparable to other research [14,45]. Although some adsorbents gave q_m values for MTP over Fe_3O_4/TiO_2/AC nanocomposite [15,46], they had various operational limitations such as tedious and expensive synthesis methods and difficult separation from the sample solution.

Table 3. The Thermodynamic Parameters Related to the MTP Adsorption on the Adsorbent

Temperature (K)	Thermodynamic parameters			
	lnK_d	ΔG (kJ mol^{-1})	ΔH° (kJ mol^{-1})	ΔS° (kJ mol^{-1} K^{-1})
298	2. 8	-7.554	-75.2	-0.227
303	2.763	-6.42		
313	1.515	-4.15		
323	0.482	-1.789		
333	-0.094	3.91		

Application of the Optimized Adsorption Method to Real Samples

To evaluate the adsorption potential of Fe_3O_4/TiO_2/AC nanocomposite, three real water samples including bottled water, tap water from Ahwaz and river Karun were studied. Real water was spiked with 10.0 and 25.0 mg l^{-1} MTP and subjected to the optimum adsorption method to study the effects of real matrices on removal efficiency. As can be seen from Table 5, removal efficiencies ranging from 95.9% to 87.8% were obtained, indicating that the adsorbent has an excellent ability to remove MTP from real water without a significant matrix effect.

Reusability Study

To evaluate the reusability of Fe_3O_4/TiO_2/AC nanocomposite, the adsorbent was reused in another

Table 4. Comparison of Adsorption Process Information of Several Adsorbents Reported in the Literature

Adsorbent	q_{max} (mg g^{-1})	T (°C)	pH	R (%)	Reusability	Ref.
AC	18.31	25	8.5	89.2	NA	[14]
Fe_3O_4@SiO_2/SiCRG[a]	447	25	7	NA[b]	3cycle	[15]
SiO_2/SiCRG	393	25	7	NA	NA	[15]
Kaolinite	17.1	NA	NA	NA	NA	[45]
Talk	10.2	NA	NA	NA	NA	[45]
Silica gel	64.8	8	5.5-8	NA	NA	[46]
Fe_3O_4/TiO_2/AC	25.32	25	8	96.2		This work

[a]k-carrageenan hybrid siliceous shells. [b]Not available.

Table 5. The Removal of MTP from Various Water Samples

Real sample	Added (mg l^{-1})	Removal (%)
Bottled water	0	-
	10.0	95.9 ± 1.5
	25.0	93.7 ± 1.7
Ahvaz tap water	0	-
	10.0	94.3 ± 2.8
	25.0	90.4 ± 1.9
Karun River	0	-
	10.0	89.3 ± 2.1
	25.0	87.8 ± 2.6

adsorption test after desorption of MTP with various solvents [46]. MTP was loaded onto 15 mg of adsorbent under optimal conditions (MTP concentration: 10 mg l^{-1} and pH 8) and magnetically separated from the sample solution. To obtain the best solvent to desorb MTP from the nanocomposite, various solvents including absolute ethanol, methanol, absolute ethanol/HCl 0.01 M mixture (80:20 v/v%), and methanol/HCl 0.01 M mixture (80:20 v/v%) were investigated. The adsorbed MTP was eluted in three consecutive steps with 0.5 ml of each solvent and then rinsed with distilled water. The results showed that the ethanol/HCl mixture was the best solvent that could almost completely remove the MTP from the adsorbent and, therefore, this solvent was selected for reusability studies. The reusability of the adsorbent was studied in the optimum conditions. The results showed that the adsorbent could be used at least three times without significant reduction in removal efficiency (Fig. S11).

CONCLUSIONS

Here, an effective approach to remove MTP from aqueous solutions with a removal efficiency of 96.2% has been developed using Fe_3O_4/TiO_2/AC nanocomposite by the adsorption process. The experimental results showed that operating factors such as the amount of adsorbent, pH, initial concentration of MTP, and temperature significantly affected the adsorption efficiency. Fe_3O_4/TiO_2/AC nanocomposite showed better performance at pH 8 and initial concentration of 10 mg l^{-1} at 25 °C. The optimum contact time of 60 min indicated that the adsorption process reaches equilibrium in a relatively short time, which can be attributed to the good adsorption tendency of the adsorbent towards MTP. Pseudo-second-order kinetic model and Freundlich isotherm were well fitted to the adsorption process. Based on these findings, it was proved that both chemical and physical adsorption mechanisms are involved in the adsorption process. The synthesized adsorbent exhibited high saturation magnetization indicating that it can be easily and quickly separated from the aqueous solution. This low-cost and non-toxic adsorbent with desirable magnetic properties showed an effective removal process under soft conditions in terms of pH and

temperature with excellent water treatment.

ACKNOWLEDGMENTS

The authors gratefully acknowledge the support of this work by Shiraz Payame Noor University research council.

REFERENCES

[1] D.B. Huggett, I.A. Khan, C.M. Foran, D. Schlenk, Environ. Pollut. 121 (2003) 199.
[2] F. Rivas, O. Gimeno, T. Borralho, M. Carbajo, J. Hazard. Mater. 179 (2010) 357.
[3] A. Piram, A. Salvador, C. Verne, B. Herbreteau, R. Faure. Chemosphere. 73 (2008) 1265.
[4] T. Deblonde, C. Cossu-Leguille, P. Hartemann. Int. J. Hyg. Environ. Health. 214 (2011) 442.
[5] R. Varga, Z. Eke, K. Torkos, Talanta 85 (2011) 1920.
[6] M.B. Ahmed, J.L. Zhou, H. H.Ngo, W. Guo, Sci. Total. Environ. 532 (2015) 112.
[7] S.F. Soares, T.R. Simoes, M. Antonio, T. Trindade, A.L. Daniel-da-Silva, Chem. Eng. J. 302 (2016) 560.
[8] A.K. Mohamed, M.E. Mahmoud, J. Molecular Liquids. 309 (2020) 113096.
[9] V. Romero, O. González, B. Bayarri, P. Marco, J. Giménez, S. Esplugas, Catal. Today 240 (2015) 86.
[10] B. Abramovic, S. Kler, D. Sojic, M. Lausevic, T. Radovic, D. Vione, J. Hazard. Mater. 198 (2011) 123.
[11] S.W. Nam, Y. Yoon, D.J. Choi, K.D. Zoh, J. Hazard. Mater. 285 (2015) 453.
[12] D. Sojic, V. Despotovic, D. Orcic, E. Szabo, E. Arany, S. Armakovic, E. Illes , K. Gajda-Schrantz , A. Dombi, T. Alapi, E. Sajben-Nagy, A. Palagyi, Cs. Vagvolgyi, L. Manczinger, L. Bjelica, B. Abramovic, J. Hydrology. 472 (2012) 314.
[13] D. Naghipour, A. Amouei, K. Taher Ghasemi, K. Taghavi, Envir. Health. Eng. Manag. J. 6 (2019) 81.
[14] S.F. Soares, T.R. Simões, M. António, T. Trindade, A. Daniel-da-Silva, Chem. Eng. J. 302 (2016) 560.
[15] F. Javier Benitez, J.L. Acero, F.J. Real, G. Roldan , E. Rodriguez, J. Chem. Technol. Biotechnol. 86 (2011) 858.
[16] M.J. Martın de Vidales, C. Saez, P. Canizares, M.A. Rodrigo, J. Chem. Technol. Biotechnol. 87 (2012) 225.
[17] J. Rivera-Utrilla, M. Sanchez-Polo, G. Prados-Joya, M.A. Ferro-Garcia, I. Bautista-Toledo, J. Hazard. Mater. 174 (2010) 880.
[18] A. Ragab, I. Ahmed, D. Bader, Molecules 24 (2019) 847.
[19] N. Kataria, V.K. Garg, Environ. Res. 172 (2019) 43.
[20] X. Wang, Y. Zhang, R. Shan, H. Hu, Ceramics Int. 47 (2021) 3219.
[21] M.R. El-Naggar, I. M. El-Naggar, M.F. El-Shahat, E.S. Abd El-Mohsen, J. Radiation Res. Applied Sciences 12 (2019) 319.
[22] A.G. El-Shamy, Polymer 202 (2020) 122565.
[23] T. Etemadinia, B. Barikbin, A. Allahresani, Surfaces Interfaces 14 (2019) 117.
[24] A.I. Abd-Elhamid, E.A. Kamoun, A.A. El-Shanshory, H.M.A. Soliman, H.F. Aly, J. Molecular Liquids 279 (2019) 530.
[25] M .Zbair, Z.Anfar, H. Ait Ahsaine, N. El Alem, M. Ezahri, J. Environ. Manag. 206 (2018) 383.
[26] N.M. Mahmoodi, M. Taghizadeh, A. Taghizadeh, J. Molecular Liquids 277 (2019) 310.
[27] I. Lung, M.L. Soran, A. Stegarescu, O. Opris, S. Gutoiu, C. Leostean, M.D. Lazar, I. Kacso, T. Da. Silipas, A.S. Porav, J. Hazard. Mater. 403 (2021) 123528.
[28] S. Kamari, A. Shahbazi, Chemosphere 243 (2020) 125282.
[29] M.E. Mahmoud, M.F. Amira, S.M. Seleim, A.K. Mohamed, J. Hazard. Mater. 381 (2020) 120979.
[30] B. Czech, K. Rubinowska, Adsorption 19 (2013) 619.
[31] M.J. Scepanovic, B. Abramovic, G. Aleksandar, S. Armakovic, J. Sol-Gel Sci. Technol. 61 (2012) 390.
[32] X. Jaramillo-Fierro, S. Gonzalez, H.A. Jaramillo, F. Medina, Nanomaterials 10 (2020) 1891.
[33] A.M. Awwad, M.W. Amer, M.M. Alaqarbeh, Chem. Inter. 6 (2020) 168.
[34] J.J. Zhang, P. Qi, J. Li, X.C. Zheng, P. Liu, X.X. Guan, G.P. Zheng, J. indust. Eng. Chem. 61(2018) 407.
[35] A. Larin, P.C. Womble, V. Dobrokhoto, Sensors 16 (2016) 1373.
[36] F.Y. Ban, S.R. Majid, N.M. Huang, H.N. Lim, Int. J. Electrochem. Sci. 7 (2012) 4345.

[37] L. Zhuang, W. Zhang, Y. Zhao1, H. Shen, H. Lin, J. Liang, Scientific Reports 5 (2015) 9320.
[38] S. Ibrahim, N. Othman, S. Sreekantan, K.S. Tan, Z. Mohd Nor, H. Ismail, Polymers 10 (2018) 1216.
[39] N. Rahbar, E. Behrouz, Z. Ramezani1, Food Anal. Methods 10 (2017) 2229.
[40] C. Yan, C. Wang, J. Yao, L. Zhang, X. Liu, Colloids Surf. A 333 (2009) 115.
[41] A.O. Dada, A.P. Olalekan, A. Olatunya, A. O. Dada, J. Appl. Chem. 3 (2012) 38.
[42] M.E. Mahmoud, M.F. Amira, M.E. Abouelanwar, S.M. Seleim, J. Mol. Liquids 299 (2019) 112192.
[43] Y. Li, Y. Wang, L. He, L. Meng, H. Lu, X. Li, J. Hazard. Mater. 383 (2020) 121144.
[44] M. Omidinasab, N. Rahbar, M. Ahmadi, B. Kakavandi, F. Ghanbari, G.Z. Kyzas, S. Silva Martinez, N. Jaafarzadeh, Environ. Sci. Poll. Res. 25 (2018) 34262.
[45] Z. Li, N.M. Fitzgerald, Z. Albert, A. Schnabl, W.T. Jiang, Chem. Eng. J. 272 (2015) 48.
[46] S. Kutzner, M. Schaffer, H. Bornick, T. Licha, E. Worch, Water Res. 54 (2014) 273.